The brain differentiates human and non-human grammars: Functional localization and structural connectivity

Angela D. Friederici, Jörg Bahlmann, Stefan Heim, Ricarda I. Schubotz, and Alfred Anwander

PNAS 2006;103;2458-2463; originally published online Feb 6, 2006;
doi:10.1073/pnas.0509389103

The brain differentiates human and non-human grammars: Functional localization and structural connectivity

Angela D. Friederici*†, Jörg Bahlmann*, Stefan Heim*‡, Ricarda I. Schubotz*, and Alfred Anwander*

*Max Planck Institute for Human Cognitive and Brain Sciences, Stephanstrasse 1a, 04103 Leipzig, Germany; and ‡Brain Mapping Group, Institute of Medicine, Research Centre Jülich, 52425 Jülich, Germany

Edited by Leslie G. Ungerleider, National Institutes of Health, Bethesda, MD, and approved December 20, 2005 (received for review October 28, 2005)

The human language faculty has been claimed to be grounded in the ability to process hierarchically structured sequences. This human ability goes beyond the capacity to process sequences with simple transitional probabilities of adjacent elements observable in non-human primates. Here we show that the processing of these two sequence types is supported by different areas in the human brain. Processing of local transitions is subserved by the left frontal operculum, a region that is phylogenetically older than Broca's area, which specifically holds responsible the computation of hierarchical dependencies. Tractography data revealing differential structural connectivity signatures for these two brain areas provide additional evidence for a segregation of two areas in the left inferior frontal cortex.

Broca's area | inferior frontal gyrus | syntax

A core component of the human language faculty is the grammatical rule system called syntax, which interplays with phonology (speech sounds) and semantics (meanings). This grammatical rule system allows the generation and understanding of an unlimited number of sentences, i.e., different combination of words, whereby the rearrangement and permutations of words in sentences are crucially licensed by hierarchical structures within the rule system (1, 2). It has been argued that the human language faculty is based on the capacity to process recursive structures (3).

Recently, it was shown that humans differ from non-human primates in their capacity to deal with hierarchically structured sequences (4). Whereas non-human primates are well set to learn and process sequences determined by local transition probabilities, e.g., a sequence like ABAB, they fail on sequences that involve more complex hierarchical structures characterized by recursive embeddings, e.g., sequences like AABB where the [AB] part is embedded, i.e., A[AB]B. The processing of such embedded structures, however, is crucial for any natural human language because they allow the understanding of embedded sentences such as "The boy [that the girl saw] was tall." Thus, it may not be surprising that humans, in contrast to non-human primates, learn and process both types of grammar, local transitions and recursive structures, with equal ease (4). These behavioral findings suggest that the evolution of the human language faculty, although building on cognitive capabilities present in our ancestors, goes far beyond these abilities.

Here the question is raised whether and how the principle processing difference between the two types of grammars is reflected in the human brain. The hypothesis is put forward that the computational requirements associated with each grammar type are reflected in a differentiated functional neuroanatomy. Two brain areas in the left frontal cortex shown to be involved in the processing of syntax are considered as prime candidate areas for such a differentiation (5). The first one is Broca's area, a phylogenetically younger region than more posteriorly and more ventrally located cortical regions, namely the ventral premotor cortex and the frontal operculum (FOP) (6). These areas have long been described to differ cytoarchitectonically (Brodmann areas, BA) according to the layering of the cortex (7). Among the six layers of the isocortex, layer IV is virtually missing in the ventral premotor cortex (BA 6). In contrast, it is present, although not fully developed, in BA 44 and fully developed in BA 45, with the two latter areas together constituting Broca's area. Therefore, the ventral premotor cortex is considered as agranular (BA 6), whereas BA 44 is classified as dysgranular and BA 45 as granular cortex (7, 8). The FOP has been described as weakly granular by some neuroanatomists (6) but has not been classified cytoarchiectronically by others (7). Today different brain areas can also be differentiated, but, moreover, receptorarchitectonically according to a different distribution of receptor binding of neurotransmitters (9). In fact, BA 6 has already been shown to differ from BA 44 and BA 45 with respect to their receptorarchitectonic characteristics (10), but the FOP remains to be specified receptorarchitectonically.

An additional possibility to structurally segregate adjacent brain regions is provided more recently by the identification of connectivity profiles based on structural imaging techniques (11, 12). Apart from allowing the segregation of adjacent brain areas, these techniques, moreover, provide information about which other brain regions a particular brain area connects (13). This information may be used to constrain interpretations of functional imaging data (12).

The hypothesis of a functional differentiation of Broca's area and the FOP is based on a review of language-related imaging studies (14). An involvement of BA 44/45 was found for the processing of sentences requiring a hierarchical reordering of the arguments due to a noncanonical surface structure (e.g., object-before-subject structure, i.e., "It was the cat that the dog chased" reordered into the subject-before-object structure, i.e., "The dog chased the cat.") or due to embedded structure (e.g., A[AB]B, i.e., "The song [that the boy sang] pleased the teacher") (15). This pattern of results was reported for English (16, 17), German (18), Hebrew (19), and Japanese (20). The processing of local structural requirements either within a phrase (21) (in German) or across adjacent phrases (22, 23) (in English) does not activate BA 44/45 but rather seems to activate the adjacent FOP. However, given that the different localizations stem from a comparison across different studies, using different paradigms, languages, and subjects, a possible functional differentiation still is a working hypothesis.

Thus the functional differentiation between BA 44/45 and FOP for grammar processing remains to be proven. If it is indeed

---

Conflict of interest statement: No conflicts declared.

This paper was submitted directly (Track II) to the PNAS office.

Abbreviations: fMRI, functional MRI; FOP, frontal operculum; FSG, Finite-State Grammar; PSG, Phrase-Structure Grammar; STG, superior temporal gyrus; TE, echo time; TR, recycle time.

†To whom correspondence should be addressed. E-mail: angelafr@cbs.mpg.de.

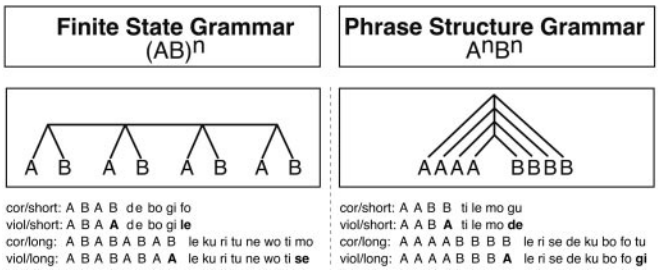

Fig. 1. Structure of the two grammar types. General structure and examples of stimuli in the FSG and PSG. Members of the two categories (A and B) were coded phonologically with category ''A'' syllables containing the vowels ''i'' or ''e'' (de, gi, le, ri, se, ne, ti, and mi) with category ''B'' syllables containing the vowels ''o'' or ''u'' (bo, fo, ku, mo, pu, wo, tu, and gu). The same syllables were used for both types of grammar. The positions of the violations in the sequences were systematically changed. Examples of correct (corr) and violation (viol, in bold) sequences are given for the short and the long condition in each grammar.

the structure of the sequence to be defined as either being hierarchical or local that determines the activation in the inferior frontal cortex, then we should observe different activations as a function of the type of sequential structure keeping everything else constant.

A functional MRI (fMRI) experiment was designed to directly test whether the two brain regions, namely BA 44/45 and FOP, can be differentiated as a function of the grammar type underlying the sequence to be computed. To this end, two grammars, allowing a direct comparison of the two functions under consideration processing structural hierarchies versus processing local probabilities, were created. Both grammar types allowed the generation of meaningless, but well structured, sequences of consonant-vowel syllables. One type of grammar is fully determined by local transitional probabilities between a finite number of items (or states) and is, therefore, called Finite-State Grammar (FSG). The other type of grammar allows the generation of phrase structures by recursive rules and is called Phrase-Structure Grammar (PSG). The ''words'' used in the two grammars were identical. The structure of the different grammars and the words used in the different classes (class A and class B) are presented in Fig. 1. Processing of each grammar type during perception requires a check of the incoming element against the predicted structure. In case of the FSG, this check is based on the evaluation of a local transition. In the case of the PSG, the prediction is based on a more elaborate process of building up hierarchical dependencies. Here we assume that the computation of hierarchical dependencies recruits BA 44/45 and that the evaluation of an incoming element against a predicted structure is supported by the FOP. The latter assumption is supported by a series of fMRI findings indicating the lateral premotor cortex to be generally involved in the evaluation of incoming elements against predicted structures in sequences (24). All subjects in both grammar groups were submitted to a learning session during which the novel grammar was learned by trial and error before scanning took place. During scanning, new correct and incorrect sequences were presented to the FSG and the PSG group, and subjects were required to judge whether a given sequence was correct with respect to the grammar they had learned.

It is worth noting that the learning that occurred before the fMRI session may draw on putative mechanisms of learning a second language although proficient use of a second language appears to be native-like. In a recent fMRI experiment on artificial grammar learning, it was shown that the initial learning phase was associated with high activation of the left hippocampus but that increased proficiency was associated with decreasing activation in the left hippocampus and an increase in the left inferior frontal gyrus (25). This finding suggests that the more proficient the language user, the more similar is the activated neural network to a native speaker (see also ref. 26).

In addition to the functional data, connectivity profiles for a subgroup of subjects were calculated for the two brain areas of interest, namely BA 44 and FOP. Under the assumption that a functional differentiation between two areas might co-occur with a differentiation of the connectivity profile of these two areas, we expected different tractograms for BA 44 and FOP.

Results

Behavioral Results. Learning of the PSG was more difficult than of the FSG (error rate of the last block of FSG, 12.1%, and of PSG, 27.0%; main effect grammar type F (1, 34) = 12.052, $P <$ 0.001). Two days later, each group was submitted to a test session during which brain activation was measured by means of MRI. Behavioral data from the present fMRI experiment revealed that the FSG was slightly easier to process (error rates for the judgment task were FSG, 6.5%, and PSG, 15.5%; main effect of grammar type: F (1, 34) = 5.01, $P < 0.05$).

Functional Imaging Results. Analyses of the BOLD contrast were performed for correct and incorrect sequences during the test session at the individual participant level and averaged over individuals for each group. Different brain activation patterns were observed for the two grammar types. Violations of either grammar caused activation in the FOP (Fig. 2 *Upper*, Talairach coordinates FSG (27): −36, 16, 0; PSG: −36, 20, −2). In contrast, only violations of PSG induced additional activation in Broca's area (Fig. 2 *Lower Right*; −46, 16, 8). Additional activation not included in the figure was found for both grammar types in the right temporal region (BA 21/22) and left BA 21 for the PSG (see Table 1). These activations are not considered to be syntax-specific, because temporal activations have been reported for both semantic and syntactic processing (15, 18). The same argumentation holds for the bilateral insula activation found for the PSG (−38, −8, 4, $z_{max} = 3.91$, $P < 0.01$; 34, 0, −2, $z_{max} = 3.60$, $P < 0.01$), as previous studies suggest that this activation is not specifically related to syntactic processing (20, 28).

An ANOVA with the factors Grammar Type (2) × Violation (2) × Length (2) × Time Step (4: 5, 7, 9, and 11 s after sequence onset) was conducted for the two critical regions of interests in the frontal cortex, FOP and Broca's area. The factor Length was included to test for the possible influence of working memory. The presence of an interaction of the factor Length and Grammar Type would indicate such an influence, the absence of such an interaction, however, indicates that the observed effects are independent of the aspect of working memory.

For the FOP, an ANOVA with the same factors revealed a significant main effect of Violation [F (1, 34) = 24.76, $P < 0.001$], Length [F (1, 34) = 5.22, $P < 0.05$], Time Step [F (3, 102) = 10.96. $P < 0.001$] and a Time Step by Length interaction [F (3, 102) = 23.82, $P < 0.001$]. The interaction was further evaluated by t tests, indicating positive values for Time Step 5 [t (18) = 6.29, $P < 0.001$] and 7 [t (18) = 2.20, $P \leq 0.05$] and negative values for the Time Steps 9 [t (18) = −4.04, $P < 0.001$] and 11 [t (18) = −5.26, $P < 0.001$]. The absence of a significant Grammar Type by Violation interaction [F (1, 34) = 1.92, not significant] indicates that the FOP subserves the processing of both the FSG and the PSG.

For Broca's area the ANOVA revealed a significant main effect of Violation [F (1, 34) = 10.36, $P < 0.01$] and Length [F (1, 34) = 10.51, $P < 0.01$] and a significant Grammar Type by Violation interaction [F (1, 34) = 4.96, $P < 0.05$]. This interaction is displayed in the time course plot for Broca's area (Fig. 2 *Lower*). It is reflected in the difference observed for the PSG between the incorrect conditions (black line for long and blue line for short sequences) and the correct conditions (green line

PSYCHOLOGY

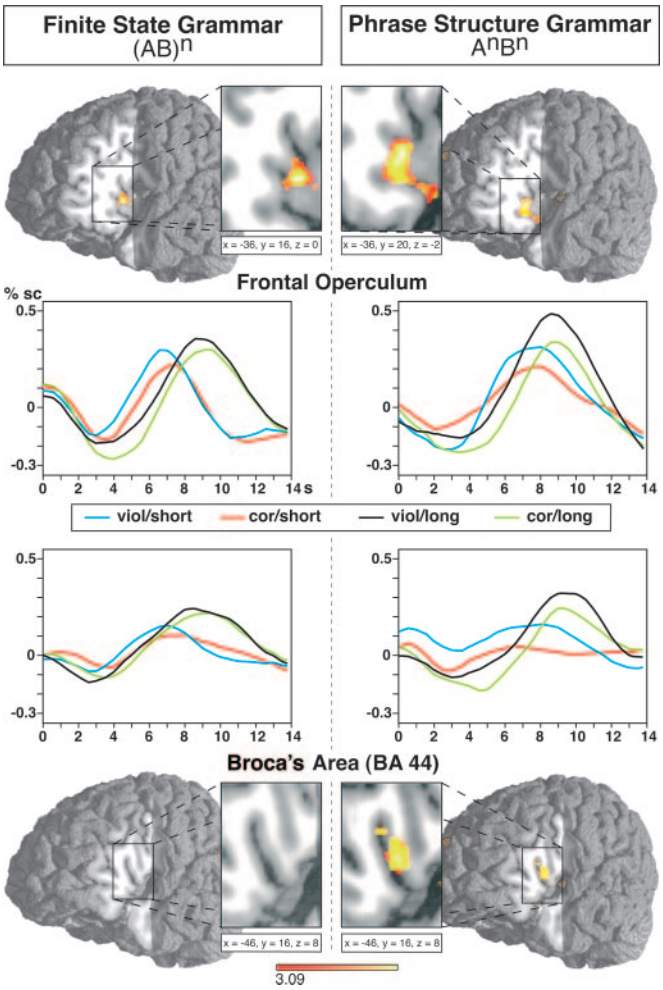

Fig. 2. Brain activation pattern for the two grammar types. Statistical parametric maps of the group-averaged activation during processing of violations of two different grammar types ($P < 0.001$, corrected at cluster level). (*Left*) The contrast of incorrect vs. correct sequences in the FSG is shown. (*Right*) The same contrast in the PSG is shown for Broca's Area (*Bottom*) and the frontal operculum (*Top*). (*Center*) Time courses (% signal change) in corresponding voxels of maximal activation are displayed.

for long and red line for short sequences). Because no such difference between incorrect and correct conditions was found for the FSG, the present data indicate that the processing of the PSG (but not of the FSG) additionally recruits Broca's area.

To demonstrate that the activity in Broca's region is not due to the difficulty of the task in the PSG, an additional analysis in BA 44/45 with the two-level factors Performance × Violation was conducted. Individual performance of the PSG group was taken into account: High performance ($n = 9$, mean value = 95% correct answers, SD = 2.8) and low performance ($n = 8$, mean value = 71% correct answers, SD = 7.4) formed the between subject factor Performance. No effect was found (Performance × Violation: $F(1, 15) = 0.47$, not significant). These results suggest that task difficulty is not correlated with the activity in Broca's area, therefore indicating the activity in Broca's area for PSG compared to FSG is to be attributed to the difference in grammar type rather than task difficulty.

Structural Imaging Results. Analysis of the diffusion tensor image data of representative subjects from the two different grammar groups reveal differential tractograms for the FOP and BA 44. In the two subjects from the FSG group who showed activation

Table 1. Talairach coordinates and *z* value for the peak location in different regions of interest for the two grammar types

Brain region	BA	Stereotactic coordinates			
		x	*y*	*z*	z_{max}
FSG					
L FOP		−36	16	0	4.15**
R superior temporal S	21/22	52	−42	2	4.41**
PSG					
L FOP		−36	20	−2	4.27**
L inferior frontal G	44	−46	16	8	3.86*
R superior temporal S	21/22	52	−40	8	4.24**
L middle temporal G	21	−46	−30	−4	3.95*

FSG (Finite-State Grammar), PSG (Phrase-Structure Grammar), and ROI (regions of interest) corresponds to a particular identified anatomical cluster (*P* value was corrected at cluster level) for the statistically significant differences of the corresponding activated regions. BA, approximate Brodmann's Area; L, left hemisphere; R, right hemisphere; G, gyrus; S, sulcus. For insular activation, see text. *, $P_{corr} = 0.01$; **, $P_{corr} = 0.001$.

in the FOP, the individual FOP activations were taken as the seed points for the individual tractograms. Both subjects demonstrated a structural connectivity of the FOP with the anterior temporal lobe via the fasciculus uncinatus (Fig. 3 *Foreground*). These connectivity profiles were also present in the two subjects from the PSG group, providing additional support for the generality of this connection (Fig. 3 *Background*). The two subjects from the PSG group had shown functional activation in Broca's area. These activations were taken as the seed points for individual tractograms. For both subjects from the PSG group, tractograms with seed points in Broca's area for these subjects indicated connectivity with the posterior and middle portion of the superior temporal region via the fasciculus longitudinalis superior (Fig. 3 *Foreground*). A look at the two subjects from the FSG group (showing no activation in BA 44) indicates that these subjects demonstrate very similar tractograms as those from the PSG group (Fig. 3 *Background*).

Thus for all four subjects, we find two distinct connectivity profiles, one connecting Broca's area via the fasciculus longitudinalis superior to the temporal lobe and one connecting the FOP via the fasciculus uncinatus to the temporal lobe. Given this structural similarity, the activation of Broca's area and the FOP, thus, is clearly a function of the input, namely the two different grammar types.

Discussion

The present results indicate a functional differentiation between two cytoarchitectonically and phylogenetically (7) different brain areas in the left frontal cortex. The evaluation of transitional dependencies in sequences generated by an FSG, a type of grammar that was shown to be learnable by non-human primates, activated a phylogenetically older cortex, the frontal operculum. In contrast, the computation of hierarchical dependencies in sequences generated according to a PSG, the type of grammar characterizing human language, additionally recruits a phylogenetically younger cortex, namely Broca's area (BA 44/45). This result is in accordance with findings across different studies showing that BA 44/45 is crucial for the processing of syntactically complex sentences hierarchies in natural languages (18, 19, 29, 30) but not for the processing of local syntactic errors (21, 22). Here we show the principal functional differentiation between BA 44/45 and FOP. Although the involvement of the FOP was observed for both grammar types, the computation of the hierarchically structured sentences only activated BA 44/45. The FOP appears to support the check of the incoming element against the predicted element and, therefore, is involved in the

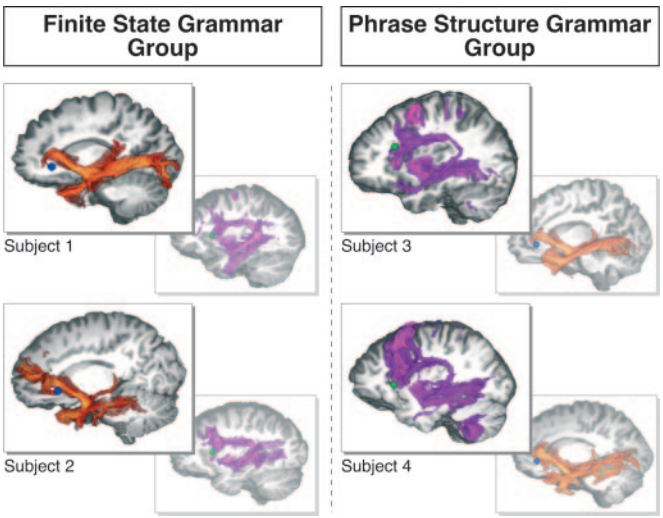

Fig. 3. Tractograms for two brain regions: Broca's area and FOP. Three-dimensional rendering of the distribution of the connectivity values of two start regions with all voxels in the brain volume (orange, tractograms from FOP; purple, tractograms from Broca's area). (*Left Foreground*) Two representative subjects of the Finite State Grammar Group with their individual activation maxima in the FOP (blue) in the critical contrast incorrect vs. correct sequences ($P < 0.005$). Talairach coordinates of Subject 1: −39, 25, 0 and Subject 2: −38, 20, −4. The individual peaks of the functional activation were taken as starting points for the tractography. For both subjects, connections to the anterior temporal lobe via the fasciculus uncinatus were detected. (*Right Foreground*) Two representative subjects of the Phrase Structure Grammar Group with their individual activation maxima in Broca's area (green) in the critical contrast incorrect vs. correct sequences ($P < 0.005$). Talairach coordinates of Subject 3: −46, 18, 21 and Subject 4: −49, 18, 4. For both subjects, the tactography detected connections from Broca's area to the posterior and middle portion of the superior temporal region via the fasciculus longitudinalis superior. (*Background*) For additional information, tractograms of each subject are given for the respective other brain area. (*Left Background*) For the FSG group, for which the FOP tracts (orange) is most relevant, Broca's area tracts (purple) are displayed. (*Right Background*) For the PSG group, for which the Broca's area tract (purple) is most relevant, FOP tracts (orange) are displayed. For these tractograms, the group mean activation voxels (see Table 1) were used as starting points.

processing of ungrammaticalities independent of the structure of the sequence. BA 44/45 is additionally recruited when structural hierarchies on which the evaluation can be based are to be computed. Importantly, our data indicate that it is not processing difficulty *per se* that causes BA 44/45 activation but that activation in this area is a function of the presence of structural hierarchies. At this point, the question arises as to what extent the computations assigned to Broca's area and FOP are specific to the language domain.

The defined areas in the inferior frontal gyrus may not be domain-specific, because, for example, Broca's area has been found to be activated when processing syntax in music (31, 32), and ventral premotor cortex was shown to be involved in monitoring stimulus for anomalies (24) by either local or global structure violation (33). Thus different brain regions may serve specific types of computations independent of the particular domains (see also ref. 34), but they appear to receive their domain specificity, however, as part of a specialized functional network.

Structural data revealed that the two functionally different areas are parts of different structural networks. Although the FOP is connected to the anterior temporal lobe via the fasciculus uncinatus, Broca's area is connected to the posterior and middle portion of the superior temporal region via the fasciculus longitudialis superior. These differential connectivity signatures receive a functional interpretation on the basis of a number of prior functional studies and the present data. The network consisting of Broca's area and the mid/posterior portion of the superior temporal gyrus (STG) was found to be activated in studies investigating syntactic complexity (18, 19) and the processing of the PSG in the present study. Activation in the posterior STG in language studies has been functionally connected to integration processes (35), because this area has been shown to be active for the processing of ungrammatical sentences where the integration of the violating element into the prior structure is impossible (21), for syntactically complex object-first sentences where the integration of the next element into the prior sentential structure is difficult (36, 37), and for sentences in which the sentence's final verb is hard to integrate because it requires a revision of the prior established argument hierarchy (38). In contrast, activation in the anterior portion of the STG together with the FOP has been reported for the processing of local phrase structure violations (21). Localization data from a magnetoencephalographic study revealed that these two activations can be functionally linked to an initial phase of structure building during which local syntactic dependencies based on word category information are checked (39). It was hypothesized that the activation of the anterior STG observed in the spoken language study may reflect access to word category information encoded in the lexicon, whereas the inferior frontal activation should be linked to the process of local structure building. Under this hypothesis, we would have expected for the present FSG activation in the FOP but not in the anterior STG. This pattern of results is what was observed in the present study.

The direct comparison of the two artificial grammar types indicates a functional differentiation of two areas in the human brain that can be differentiated phylogenetically (7), cyto- and receptorarchitectonically (8–10), and with respect to their structural connectivity signatures (present data). The observation that the grammar type processed by human and non-human primates is subserved by a brain area, which is phylogenetically older than the brain area subserving the processing of the grammar type only learnable by humans, may be interpreted to reflect an evolutionary trait in the phylogeny from non-human to human primates. However, a direct comparison at the neuroarchitectonic level appears to be premature at present because although a subdivision of the prefrontal cortex in the macaque monkey has been proposed both on cytoarchitectonic (40) and on functional data (41), the homologies between the monkey and the human cortex are still under discussion. Therefore, presently, it is unclear whether F5 in the macaque has to be considered as the precursor of human BA 44 or whether F5 has to be viewed as the direct precursor of human BA 6, whereas BA 44 (already present with a maximal width of 4–9 mm in the macaque) evolved into the larger BA 44 in humans (42).

In conclusion, there is no doubt that processing syntactic hierarchies and recursion is a crucial aspect of human language. Although some take it to be one of several crucial aspects (43), others consider it as the only aspect that makes human language special (3). Here we report findings pointing toward an evolutionary trajectory with respect to the computation of sequences, from processing simple probabilities to computing hierarchical structures, with the latter recruiting Broca's area, a cortical region that is phylogenetically younger than the frontal operculum, the brain region dealing with the processing of transitional probabilities.

Methods

Participants. Forty healthy, right-handed subjects participated in this study (19 male, mean age 26 years, SD = 2.7 years). They were native German speakers and had normal or corrected to normal vision. No subject had a known history of neurological, major medical, or psychiatric disorder. Before scanning, subjects were informed about the potential risks and gave a declaration of consent.

Stimuli. Sequences of consonant-vowel syllables were visually presented to the subjects. The syllables were assigned to two classes (A and B), which were coded by different consonants and vowels (see Fig. 1). For both types of artificial grammar, the same syllables were used. The probability of occurrence of the frequency of the several syllables was balanced to prevent pattern learning. If one syllable would occur by chance more frequently in a certain position of one sequence, the subject could assume a rule behind this chunk. Hence, all syllables appeared with equal frequency in the experiment.

Violations occurred at different positions in the sequence, thus forcing the subjects to parse the entire sequences according to the rule as learned. Violations occurred at positions in the four-element short sequences and at the crucial positions 1, 2, 7, and 8 in the eight-element long sequences for the FSG and at the positions 1, 8, 4, and 5 in the long sequences for the PSG (compare structures in Fig. 1). To process these sequences, subjects had to judge their grammaticality, identify the class membership of a given consonant-vowel-syllable, and match the class membership of the incoming element with the rule-based predicted class.

Procedure. Subjects were randomly assigned to one of two groups either by learning FSG or PSG. A between-subject design was chosen to prevent interference of the two grammars during learning and testing.

Learning. Learning took place 2 days before the fMRI experiment. The learning period was segmented into 12 blocks. In each block, 10 correct sequences were presented. Thereafter, five correct and five incorrect sequences were shown. Participants were instructed to extract the rule underlying the syllable sequences. In total, 240 stimuli were presented. Sequences of four, six, and eight syllables were used in both the FSG and the PSG; i.e., FSG: $(AB)^2$, $(AB)^3$, $(AB)^4$; PSG: A^2B^2, A^3B^3, A^4B^4 (80 items each). Sequences of each grammar type were presented visually. Subjects were required to respond to sequences by indicating with a button press whether the sequences were grammatical or ungrammatical. Feedback was given. The learning lasted 23 min.

Testing. In the fMRI session, 160 new items were presented (80 correct and 80 incorrect). Half of the sequences contained four syllables, and half of them eight syllables. Sequences of two different lengths were included to allow for a possible influence of working memory under the assumption that short sequences (four elements) require less working memory than long sequences (eight elements). This consideration should hold in particular for sequences of PSG. Subjects judged whether the sequences were rule-based. Again, feedback was given. 40 null events were included and presented in a pseudorandomized order with the other trials.

Each sequence started with a fixation cross (500 ms). Each syllable was presented for 300 ms with an interstimulus interval of 200 ms between the syllables. Then, subjects could respond for 1,000 ms, followed by feedback for 500 ms. Trials started with a jitter of 0, 500, 1,000, or 1,500 ms.

fMRI Data Acquisition. Imaging was performed on a 3T Trio scanner (Siemens, Erlangen, Germany) equipped with the standard birdcage head coil. Stabilization cushions were used to reduce head motion. For registration purposes, two sets of two-dimensional anatomical images were acquired for each participant immediately before the functional imaging. A Modified Driven Equilibrium Fourier Transform and an EPI-T1 sequence were used. T1-weighted Modified Driven Equilibrium Fourier Transform (44) images [data matrix 256×256, recycle time (TR) = 1.3 s, echo time (TE) = 7.4 ms] were obtained with a non-slice-selective inversion pulse followed by a single excitation of each slice (45). Anatomical images were positioned parallel to anterior commissure-posterior commissure. Functional data were acquired from 16 axial slices (thickness = 3 mm; gap = 0.6 mm) by using a gradient-echo planar imaging with a TE of 30 ms, flip angle of 90°, TR of 2.000 ms, and acquisition bandwidth of 100 kHz. The matrix acquired was 128×128 with a field of view of 25.6 cm, resulting in an in-plane resolution of 2 mm $\times$ 2 mm. One functional run with 666 time points was measured.

Functional Imaging Data Analysis. The fMRI data processing was performed by using the software package LIPSIA (46). Functional data were motion-corrected offline with the Siemens motion correction protocol (Siemens). To correct for the temporal offset between the slices acquired in one scan, a cubic-spline-interpolation was applied. A temporal highpass filter with a cutoff frequency of 1/60 Hz was used for baseline correction of the signal, and a spatial Gaussian filter with 3.768 mm full width at half maximum was applied. The increased autocorrelation caused by the filtering was taken into account during statistical calculation by an adjustment of the degrees of freedom. To align the functional slices with a 3D stereotactic coordinate reference system, a rigid linear registration with six degrees of freedom (three rotational and three translational) was performed. The rotational and translational parameters were acquired on the basis of the Modified Driven Equilibrium Fourier Transform and EPI-T1 slices to achieve an optimal match between these slices and the individual 3D reference data set. This 3D reference data set was acquired for each subject during a previous scanning session. The Modified Driven Equilibrium Fourier Transform volume data set with 160 slices and 1-mm slice thickness was standardized to the Talairach stereotactic space (27). The rotational and translational parameters were subsequently transformed by linear scaling to a standard size. The resulting parameters were then used to transform the functional slices by using trilinear interpolation so that the resulting functional slices were aligned with the stereotactic coordinate system. This linear normalization process was improved by a subsequent processing step that performed an additional nonlinear normalization.

The statistical evaluation was based on a least-squares estimation by using the general linear model for serially autocorrelated observations (47, 48). The design matrix was generated with a synthetic hemodynamic response function (49) and its first and second derivative. The model equation, including the observation data, the design matrix, and the error term, was convolved with a Gaussian kernel of dispersion of 4 s full width at half maximum to deal with the temporal autocorrelation (50). Contrast images of the differences between the specified conditions were calculated for each subject. Each individual functional data set was aligned with the standard stereotactic reference space. Because of poor behavioral data in the fMRI session ($<57\%$ correct answers), three subjects were excluded from the analysis. Group analyses (random-effects model) based on the contrast images were subsequently performed. The individual contrast images were then entered into a second-level random effects analysis (one-sample t test). Subsequently, t values were transformed into Z scores. To protect against false-positive activations, only regions with a Z score >3.09 ($P < 0.05$; corrected for multiple comparisons) and with a volume >120 mm^3 (10 voxels) were considered.

The time course analysis for the region-of-interest in the FOP was performed in the voxel (x, y, and z of the Talairach system), yielding the highest activation (contrast incorrect vs. correct) in both the PSG and the FSG group (-34, 20, -2). For the region-of-interest in Broca's area, the highest activated voxel in the PSG (-46, 16, 8) was chosen, and time courses were calculated for both groups at this voxel coordinate.

Structural Data Acquisition. Diffusion-weighted data and high-resolution 3-D T1-weighted as well as 2D T2-weighted images were acquired in four subjects (two from the FSG and two from the PSG group) on a Siemens 3T Trio Scanner with an eight-channel array head coil.

The diffusion-weighted data were acquired by using a spin-echo EPI sequence (TR = 8.100 ms, TE = 120 ms, 44 axial slices, resolution 1.7 × 1.7 × 3.0 mm, gap = 0.3 mm, two acquisitions, maximum gradient strength 40 mT/m). The diffusion weighting was isotropically distributed along 24 directions (b value = 1,000 s/mm^2). Additionally a data set with no diffusion weighting was acquired. The total scan time was ≈7 min.

The T2-weighted images (RARE; TR = 7,800 ms; TE = 105 ms, 44 axial slices, resolution 0.7 × 0.7 × 3.0 mm, gap = 0.3 mm, flip angle 150°) were coregistered to the 3D T1-weighted (MPRAGE; TR = 100 ms, TI = 500 ms, TE = 2.96 ms, resolution 1 × 1 × 1 mm, flip angle 10°, two acquisitions) images. Subsequently, the diffusion-weighted images were nonlinearly registered onto the T2-weighted images to reduce distortion artifacts. Based on the registered diffusion weighted images, a diffusion tensor image was calculated.

White Matter Tractography. For diffusion tensor image analysis, we developed a 3D extension of the random walk method proposed by Koch *et al.* (51). The algorithm was applied to all white matter voxels in the functional activated area. The target space for the tractography was the whole white matter volume with a resolution of 1 × 1 × 1 mm. The fiber tracts for all start voxels in the region were averaged.

The algorithm can be described by a model of particles, moving randomly from voxel to voxel. The transition probability to a neighboring voxel depends on a local probability density function based on the local diffusivity profile that is modeled from the diffusion tensor image measurement. The particle will move with a high probability along directions with high diffusivity, i.e., the presumed fiber direction. While repeating this random walk many times, we get a relative measure of the anatomical connectivity between the start and the target voxel. For each elementary transition, the probability for a movement is computed from the product of the diffusion coefficient of the two neighboring voxels in the direction of the connecting line. The product is raised to the 7th power to focus the probability distribution to the main fiber direction and suppress the influence of transverse diffusion. This value was empirically chosen in such a way that the trajectories of most particles follow the main fiber directions. A total of 500,000 particles were tested for the start region. To compensate for the distance-dependent bias of connectivity, each value is normalized to the distance to the start region. After reducing the dynamic range of the connectivity values by logarithmic transformation, the values were scaled to the range between 0 and 1. To remove random artifacts, only voxels with connectivity values >0.6 were displayed. This 3D distribution of connectivity values in the brain is called tractogram.

We thank W. Tecumseh Fitch for discussions on the work presented in this manuscript and D. Yves von Cramon for providing his neuroanatomical expertise.

1. Chomsky, N., ed. (1957) *Syntactic Structures* (Mouton, The Hague, The Netherlands).
2. Chomsky, N. (1959) *Inf. Contr.* **2,** 91–112.
3. Hauser, M. D., Chomsky, N. & Fitch, W. T. (2002) *Science* **298,** 1569–1579.
4. Fitch, W. T. & Hauser, M. D. (2004) *Science* **303,** 377–380.
5. Friederici, A. D. (2004) *Trends Cogn. Sci.* **8,** 245–247.
6. Sanides, F. (1962) *Die Architektonik des menschlichen Stirnhirns* (Springer, Berlin).
7. Brodmann, K. (1909) *Vergleichende Lokalisationslehre der Großhirnrinde* (J.A. Barth, Leipzig, Germany).
8. Amunts, K., Schleicher, A., Burgel, U., Mohlberg, H., Uylings, H. B. & Zilles, K. (1999) *J. Comp. Neurol.* **412,** 319–341.
9. Zilles, K., Schleicher, A., Palomero-Gallagher, N. & Amunts, K. (2002) in *Brain Mapping: The Methods*, eds. Mazziotta, J. C. & Toga, A. (Elsevier, San Diego), pp. 573–602.
10. Amunts, K. & Zilles, K. in *Broca's Region*, eds. Grodzinsky, Y. & Amunts, K. (Oxford Univ. Press, Oxford), in press.
11. Behrens, T. E., Johansen-Berg, H., Woolrich, M. W., Smith, S. M., Wheeler-Kongshott, C. A., Boulby, P. A., Barker, G. J., Sillery, E. L., Sheehan, K., Ciccarelli, O., *et al.* (2003) *Nat. Neurosci.* **6,** 750–757.
12. Johansen-Berg, H., Behrens, T. E. J., Robson, M. D., Drobnjak, I., Rushworth, M. F. S., Brady, J. M., Smith, S. M., Higham, D. J. & Matthews, P. M. (2004) *Proc. Natl. Acad. Sci. USA* **101,** 13335–13340.
13. Catani, M., Jones, D. K. & Ffytche, D. H. (2005) *Ann. Neurol.* **57,** 8–16.
14. Friederici, A. D. (2002) *Trends Cogn. Sci.* **6,** 78–84.
15. Kaan, E. & Swaab, T. Y. (2002) *Trends Cogn. Sci.* **6,** 350–356.
16. Stromswold, K., Caplan, D., Alpert, N. & Rauch, S. (1996) *Brain Lang.* **52,** 452–473.
17. Peelle, J. E., McMillan, C., Moore, P., Grossman, M. & Wingfield, A. (2004) *Brain Lang.* **91,** 315–325.
18. Röder, B., Stock, O., Neville, H., Bien, S. & Roesler, F. (2002) *NeuroImage* **15,** 1003–1014.
19. Ben-Shachar, M., Hendler, T., Kahn, I., Ben-Bashat, D. & Grodzinsky, Y. (2003) *Psychol. Sci.* **14,** 433–440.
20. Musso, M., Moro, A., Glauche, V., Rijntjes, M., Reichenbach, J., Büchel, C. & Weiller, C. (2003) *Nat. Neurosci.* **6,** 774–781.
21. Friederici, A. D., Rüschemeyer, S.-A., Hahne, A. & Fiebach, C. J. (2003) *Cereb. Cortex* **13,** 170–177.
22. Ni, W., Constable, R. T., Mencl, W. E., Pugh, K. R., Fulbright, R. K., Shaywith, B. A., Gore, J. C. & Shankweiler, D. (2000) *J. Cogn. Neurosci.* **12,** 120–133.
23. Opitz, B. & Friederici, A. D. (2004) *J. Neurosci.* **24,** 8436–8440.
24. Schubotz, R. I. & von Cramon, D. Y. (2003) *NeuroImage* **20,** S120–S131.
25. Opitz, B. & Friederici, A. D. (2003) *NeuroImage* **19,** 1730–1737.
26. Wartenburger, I., Heekeren, H. R., Abutalebi, J. Cappa, S. F., Villringer, A. & Perani, D. (2003) *Neuron* **37,** 159–170.
27. Talairach, P. & Tournoux, J., eds. (1988) *A Stereotactic Coplanar Atlas of the Human Brain* (Thieme, Stuttgart, Germany).
28. Kuperberg, G. R., McGuire, P. K., Bullmore, E. T., Brammer, M. J., Rabe-Hesketh, S., Wright, I. C., Lythgoe, D. J., Williams, S. C. & David, A. S. (2000) *J. Cogn. Neurosci.* **12,** 321–341.
29. Tettamanti, M., Alkadhi, H., Moro, A., Perani, D., Kollias, S. & Weniger, D. (2002) *NeuroImage* **17,** 700–709.
30. Grodzinsky, Y. (2000) *Behav. Brain Sci.* **23,** 1–21.
31. Maess, B., Koelsch, S., Gunter, T. C. & Friederici, A. D. (2001) *Nat. Neurosci.* **4,** 540–545.
32. Koelsch, S., Gunter, T. C., von Cramon, D. Y., Zysset, S., Lohmann, G. & Friederici, A. D. (2002) *NeuroImage* **17,** 956–966.
33. Schubotz, R. I. & von Cramon, D. Y. (2002) *NeuroImage* **15,** 787–796.
34. Scott, S. K., Blank, C. C., Rosen, S. & Wise, R. J. S. (2000) *Brain* **123,** 2400–2406.
35. Friederici, A. D. & Kotz, S. A. (2003) *NeuroImage* **20,** S8–S17.
36. Cooke, A., Zurif, E. B., DeVita, C., Alsop, D., Koenig, P., Detre, J., Gee, J., Pinango, M., Balogh, J. & Grossman, M. (2002) *Hum. Brain Mapp.* **15,** 80–94.
37. Constable, R. T., Pugh, K. R. Berroya, E., Mencl, W. E., Westerveld, M., Ni, W. & Shankweiler, D. (2004) *NeuroImage* **22,** 11–21.
38. Bornkessel, I., Zyssett, S., Friederici, A. D., von Cramon, D. Y. & Schlesewsky, M. (2005) *NeuroImage* **26,** 221–233.
39. Friederici, A. D., Wang, Y., Herrmann, C. S., Maess, B. & Oertel, U. (2000) *Hum. Brain Mapp.* **11,** 1–11.
40. Petrides, M. & Pandya, D. N. (1994) in *Handbook of Neuropsychology*, eds. Boller, F. & Grafman, J. (Elsevier, Amsterdam), pp. 17–58.
41. Rizzolatti, G. & Luppino, G. (2001) *Neuron* **31,** 889–901.
42. Petrides, M., Cadoret, G. & Mackey, S. (2005) *Nature* **435,** 1235–1238.
43. Pinker, S. & Jackendoff, R. (2005) *Cognition* **95,** 201–236.
44. Ugurbil, K., Garwood, M., Ellermann, J., Hendrich, K., Hinke, R., Hu, X. P., Kim, S. G., Menon, R., Merkle, H., Ogawa, S., *et al.* (1993) *Magn. Reson. Q.* **9,** 259–277.
45. Norris, D. G. (2000) *J. Magn. Reson. Imaging* **11,** 445–451.
46. Lohmann, G., Müller, K., Bosch, V., Menthel, H., Hessler, S., Chen, L., Zysset, S. & von Cramon, D. Y. (2001) *Comput. Med. Imaging Graph.* **25,** 449–457.
47. Friston, K. J. (1994) in *Functional Neuroimaging*, eds. Thatcher, R. W., John, E. R. & Hallett, M. (Academic, San Diego), pp. 79–93.
48. Friston, K., Holmes, A. P., Worsley, K. J., Poline, J.-P., Frith, C. D. & Frackowiak, R. S. J. (1995) *Hum. Brain Mapp.* **2,** 189–210.
49. Worsley, K. J. & Friston, K. J. (1995) *NeuroImage* **2,** 173–181.
50. Friston, K. J., Fletcher, P., Josephs, O., Homes, A., Rugg, M. D. & Turner, R. (1998) *NeuroImage* **7,** 30–40.
51. Koch, M. A., Norris, D. G. & Hund-Georgiadis, M. (2002) *NeuroImage* **16,** 241–250.